RSC Advances

PAPER

View Article Online
View Journal | View Issue



Cite this: RSC Adv., 2015, 5, 27330

# Synthesis and tensioactive properties of PEO-*b*-polyphosphate copolymers†

S. Vanslambrouck,[ac] B. Clément,[ac] R. Riva,[a] L. H. Koole,[b] D. G. M. Molin,[c] G. Broze,[a] P. Lecomte[ac] and C. Jérôme*[ac]

Received 20th February 2015
Accepted 10th March 2015

DOI: 10.1039/c5ra02205c

www.rsc.org/advances

Poly(ethylene oxide) (PEO)-*b*-polyphosphate copolymers made of hydrophilic PEO and hydrophobic polyphosphates are amphiphilic copolymers prone to self-assemble in water into nanoparticles. In this work, nanoparticles are obtained by the self-assembly of PEO-*b*-polyphosphate copolymers in water in the absence of any organic co-solvent whatever the length of the pendant alkyl chain (between 4 and 7 carbon atoms) of the polyphosphate block. Remarkably, this solvent-free process remains efficient even for the most hydrophobic polyphosphate blocks. The critical aggregation concentration (CAC) of the block copolymers was determined by pyrene probe fluorescence. Finally, the efficiency of these copolymer surfactants to decrease the air–water interface was measured by air-bubble tensiometry.



## Introduction

Amphiphilic block copolymers hold a special place in macromolecular chemistry due to their dual nature with one block exhibiting hydrophilicity and the other one lipophilicity. They are widely used in diverse applications,[1,2] including detergency,[3] dispersion and foam stabilization[4,5] and drug delivery systems[6] in which they demonstrated some advantages such as a lower critical micellar concentration as compared to small size surfactants. These copolymers are able to self-assemble in water, driven primarily by the hydrophobic effect but also by electrostatic interactions, inclusion complexes and hydrogen bonding.

The self-assembly of few non-ionic amphiphilic copolymers was investigated compared to the cationic, anionic, or amphoteric ones. Among the non-ionic copolymers displaying micellization ability, the majority of the research was performed on poly(ethylene oxide) (PEO) as the hydrophilic block with poly(propylene oxide) (commercially called "Pluronics")[7,8] or degradable aliphatic polyesters, *i.e.* poly(ε-caprolactone)[9,10] (PCL) and poly(lactide)[11] (PLA) as the hydrophobic block.[12] Indeed, such PEO-based non-ionic surfactants being biocompatible and less toxic than ionic ones were extensively investigated for diverse oral and parenteral pharmaceutical formulations.[13,14] A well-known example is Tween-80 which is less toxic, less haemolytic and maintains nearly physiological pH in solution.[15]

At the end of the 1970s, Penczek and co-workers achieved a pioneering work establishing that polyphosphates can be synthesized by ring-opening polymerization (ROP) of cyclic phosphates.[16,17] Organometallic compounds such as aluminum alkoxides[18] and tin octanoate ($Sn(Oct)_2$)[19] are commonly used to promote the ROP of cyclic phosphates. Nowadays these metal-based promoters are replaced by metal-free organocatalysts.[20,21] Similarly to aliphatic polyesters (PCL, PLA,…), polyphosphates are degraded by reaction with water. Indeed, Baran and Penczek showed that the kinetics of the polyphosphates hydrolytic degradation is affected by a number of parameters, such as temperature, pH and chemical structure of the pendant chains.[22] Narendran and Kishore reported on a series of polyphosphates that exhibit a faster hydrolytic degradation at basic pH, leading to a weight loss of 3.9% in six hours (for the most stable polymer).[23] Wang *et al.* described a slower hydrolytic degradation for a PEO-*b*-polyphosphate amphiphilic block copolymers at 37 °C and pH 7.4 in a phosphate buffer solution (a weight loss of 7% for the polyphosphate block in two months).[24] Consequently, polyphosphates turned out to be a valuable alternative to aliphatic polyesters as a degradable hydrophobic polymers for the elaboration of diblock amphiphilic polymers. In terms of applications, these polyphosphates appear particularly appealing for the fabrication of surfactants or nanocarriers in the field of Drug Delivery systems.[25–28]

In contrast to aliphatic polyesters, the chemical structure of polyphosphates is easily changed by simple modification of lateral groups. This task is achieved by the implementation of the ROP of cyclic phosphates prepared by the esterification reaction of 2-chloro-1,3,2-dioxaphospholane 2-oxide (COP) with the appropriate alcohol (Scheme 1).[29,30] This strategy was applied by Yang *et al.* in order to modify the hydrophobicity of the polyphosphate block of amphiphilic copolymers.[31] It turned

[a]Center for Education and Research on Macromolecules, University of Liege, Chemistry Department, B6a, Sart-Tilman, B-4000 Liege, Belgium. E-mail: c.jerome@ulg.ac.be
[b]Faculty of Health, Medicine and Life Science, Department of Biomedical Engineering/Biomaterials Sciences, Maastricht University, Maastricht, The Netherlands
[c]BioMIMedics, Interred EMR IV-A Consortium: Lead Partner Maastricht University, Universiteitssingel 50, 6229ER Maastricht, The Netherlands

† Electronic supplementary information (ESI) available: See DOI: 10.1039/c5ra02205c

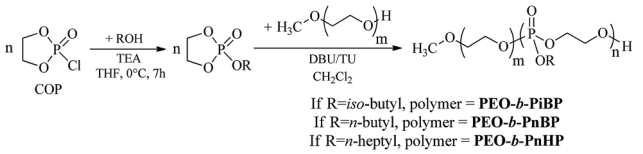


Scheme 1 Followed strategy for the synthesis of the PEO-*b*-polyphosphate copolymers.



out that the longer the lateral chains are, the more hydrophobic the polyphosphate block is and the lower the Critical Aggregation Concentration (CAC) is. Nevertheless, in their work, the nanoparticles were prepared by dropwise addition of water into a solution of the amphiphilic diblock copolymer in an organic solvent (DMSO). The higher hydrophilicity of polyphosphates compared to aliphatic polyesters opens up the possibility to exploit them to prepare nanoparticles in the absence of any potentially toxic organic solvent,[32] which is an important advantage for several applications and especially for food, biomedical and detergency applications.

Our work aims at investigating the self-assembly without addition of organic co-solvent of PEO-*b*-polyphosphate copolymers in water and at the air–water interface. For this purpose, PEO-*b*-polyphosphate copolymers of increasing hydrophobicity by increasing the number of carbon atoms of pendant group were synthesized according to a similar strategy used by Yang *et al.*[31] Besides the length, the effect of the alkyl group architecture was investigated on the CAC of the block copolymers determined by pyrene probe fluorescence. Finally, the efficiency of these copolymer surfactants to decrease the air–water interface was measured by air-bubble tensiometry.

## Results and discussion

The first step of our work is dedicated to the synthesis of PEO-*b*-polyphosphate copolymers. It was decided to use polyphosphates substituted by pendant *n*-butyl, iso-butyl and *n*-heptyl groups. The use of the ethyl group was discarded because of the known hydrosolubility of the corresponding polyphosphate,[33] which is not suitable as the hydrophobic block for our study. On the one side, polymers substituted by the *n*-butyl and iso-butyl groups were selected in order to investigate the influence of the branching on the self-assembly of the corresponding amphiphilic copolymers in water. The *tert*-butyl group was discarded because such tertiary carbon could affect the stability of the resulting phosphate towards hydrolysis. On the other side, the comparison of the self-assembly of copolymers bearing pendant *n*-butyl and *n*-heptyl groups enabled the investigation of the effect of the length of the substituent in the absence of any organic co-solvent.

### Monomer synthesis

The synthesis of cyclic phosphates is described in many works.[21,31] Briefly, the cyclic phosphates substituted by a *n*-butyl group (*n*BP), an iso-butyl group (iBP) or a *n*-heptyl group (*n*HP) were synthesized by the esterification reaction of the commercially available COP and the corresponding alcohol (1-butanol, iso-butanol or 1-heptanol) in the presence of a stoichiometric amount of TEA at 0 °C for 7 hours (Scheme 1).

After filtration of the released triethylammonium hydrochloride salt, the monomers were purified by fractionated distillation under vacuum with an average final yield of 60% for *n*BP and iBP monomers and 50% for *n*HP. The structure of the different monomers was assessed by $^1$H NMR, by $^{13}$C NMR and by $^1$H-decoupled $^{31}$P NMR analyses (see in the ESI†).

### Synthesis of PEO-*b*-polyphosphate amphiphilic copolymers

Generally, hydrophilic PEO is used to synthesize non-ionic amphiphilic copolymers. Among the degradable amphiphilic copolymers, PEO-*b*-PCL copolymers are one of the most described in the scientific literature. Previous researches reported a molar mass of 5000 g mol$^{-1}$ as typical interesting length for the PEO block of such surfactant copolymer,[31,34,35] notable because of the possible renal extraction when use in pharmaceutical fields.[36] For sake of comparison, this length was selected for the PEO macroinitiator. Besides, a polymerization degree of 10 was targeted for each polyphosphate block for the sake of comparison with more commonly used $PEO_{114}$-*b*-$PCL_8$ copolymer surfactants.

Accordingly, the synthesis of $PEO_{114}$-*b*-$PiBP_{10}$, $PEO_{114}$-*b*-P*n*$BP_{10}$ and $PEO_{114}$-*b*-P*n*$HP_{10}$ copolymers was investigated by organocatalyzed ROP of cyclic phosphates in living conditions, by using monomethoxypoly(ethylene oxide) (MeO-PEO-OH) (5000 g mol$^{-1}$) as macro-initiator. From literature data,[21] a mixture of 1,8-diazabicyclo[5.4.0]undec-7-ene (DBU) and 1-1-[3,5-bis(trifluoromethyl)phenyl]-3-cyclohexyl-2-thiourea (TU) appears as one of the most efficient catalytic system for polymerizing related cyclic phosphates. Based on these conditions ($CH_2Cl_2$, 0 °C and 60 min for iBP and *n*BP monomers or 70 min for *n*HP monomer), the monomer to macro-initiator ratio was set to 10 and polymerization let to full conversion. Accordingly, the three targeted amphiphilic copolymers were successfully obtained in a controlled fashion as depicted by the good agreement between the theoretical and experimental molar masses for each copolymer (Table 1) and the narrow molecular weight distribution. The structures of the different PEO-*b*-polyphosphate copolymers and the molar masses of the corresponding polyphosphate block were determined by $^1$H NMR analysis. The typical $^1$H NMR spectrum of PEO-*b*-P*n*HP is shown Fig. 1 and $M_{n\mathrm{HP}}$ = 222 g mol$^{-1}$ ($M_{\mathrm{iBP}} = M_{n\mathrm{BP}}$ = 180 g mol$^{-1}$).

The molar mass of the P*n*HP block was measured by the comparison of the intensity of the signal of the PEO block at 3.6 ppm (Fig. 1, peak C) and the typical signal of polyphosphate block at 1.3 ppm (Fig. 1, peak F) according to eqn (1), where $I_C$ and $I_F$ stand for the integral of the C and F peaks in Fig. 1.

$$M_{\mathrm{n,NMR}}(\mathrm{P}n\mathrm{HP\ block}) = \mathrm{DP_{PEO}} \times \frac{I_F}{2I_C} \times M_{\mathrm{monomer}} \quad (1)$$

Table 1 Macromolecular characteristics of the different PEO-*b*-polyphosphate amphiphilic copolymers

| Monomer | Catalyst DBU/TU ratio (mmol) | Polym. time (min) | $M_{n,PEO}$ macroinitiator (g mol$^{-1}$) | $DP_{theo}$ PPhos | $M_{n,theo}$[a] PPhos (g mol$^{-1}$) | $DP_{exp}$[b] PPhos | $M_{n,NMR}$[b] PPhos (g mol$^{-1}$) | $M_{n,SEC}$[c] total (g mol$^{-1}$) | $M_w/M_n$[c] | HLB[d] |
|---|---|---|---|---|---|---|---|---|---|---|
| iBP | 2.7/1.2 | 60 | 5000 | 10 | 1800 | 8 | 1500 | 5200 | 1.10 | 15.4 (18.6) |
| *n*BP | 2.7/1.2 | 60 | 5000 | 10 | 1800 | 9 | 1600 | 5300 | 1.10 | 15.2 (18.4) |
| *n*HP | 2.7/1.2 | 70 | 5000 | 10 | 2200 | 8 | 1800 | 5700 | 1.10 | 14.7 (17.6) |

[a] Theoritical value for the molar mass of the polyphosphate block determined by the initial monomer/initiator ratio. [b] Polymerization degree and molar mass of the polyphosphate block determined by $^1$H NMR according eqn (1). [c] Molar mass (calculated for the main peak) and molar mass distribution (calculated for the entire elugram) of the diblock copolymers determined by SEC in THF (PEO standards). [d] HLB calculated by the Griffin equation $20 \times [1 - M_n(\text{hydrophobic block})/M_n(\text{total})]$ considering the phosphate block as hydrophobic, in bracket, HLB calculated by considering only the alkyl group as hydrophobic.

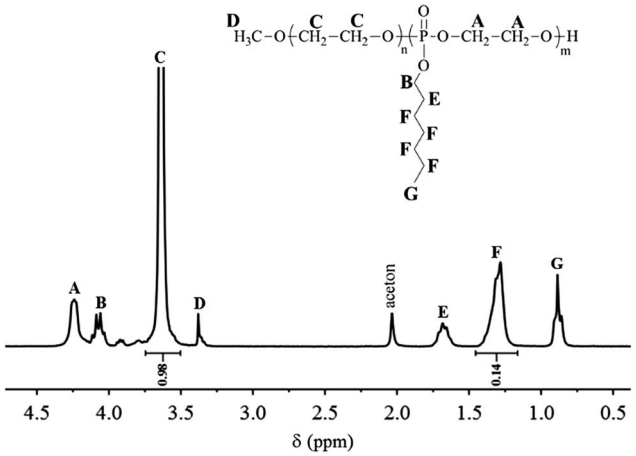


Fig. 1 $^1$H NMR spectrum of PEO-*b*-P*n*HP copolymer in $CDCl_3$.

The $^1$H-decoupled $^{31}$P NMR spectrum (see ESI†) of the PEO-*b*-P*n*HP copolymer confirmed the complete conversion of *n*HP monomer into the corresponding polymer by the shift of the signal from 18 ppm to −1 ppm.

SEC analysis confirmed also the success of the block copolymerization. Indeed, after polymerization, a shift of the PEO macro-initiator traces to higher apparent molar mass is observed in each case (Fig. 2). Moreover, no trace of residual PEO is observed, which is in good agreement with a quantitative initiation by the PEO macro-initiator.

However, although the SEC trace of MeO-PEO-OH is monomodal, the SEC traces of the three different PEO-*b*-polyphosphate copolymers are bimodal. Indeed, a second population is observed at higher molar masses, which was attributed to the presence of a triblock copolymer, polyphosphate-*b*-PEO-*b*-polyphosphate coming from the unavoidable initiation of the cyclic phosphate polymerization by HO-PEO-OH, present in small amount in the commercial MeO-PEO-OH. The separation of these copolymer mixtures being tedious, they have been used without further purification for the following step, knowing that it represents about 10% of the sample.

## Aqueous behaviour of PEO-*b*-polyphosphate diblock copolymers

The main step of our work is to investigate the self-assembly of the diblock copolymers in water without the use of organic co-solvent. Indeed, the water contact angles of films of P*n*BP and P*n*HP homopolymers (~10.000 g mol$^{-1}$) were measured to be 7.6° and 14.8°, respectively (experimental details provided in ESI†), showing the high hydrophilic character of these polyphosphates, even if both homopolymers are insoluble in water at room temperature. This fact in combination with the low $T_g$ (<−50 °C) and the absence of crystallinity observed for the polyphosphate block of the copolymers, in contrast to the semi-crystalline PCL, would favour such solvent-free process (DSC traces of the amphiphilic copolymers are provided as ESI†).

The self-assembly of amphiphilic copolymers depends on the hydrophilic-lipophilic balance (HLB), usually calculated by the Griffin equation. HLB calculated by considering as the hydrophobic segments the only alkyl side-chain (10 butyl or 10 heptyl), and keeping the polyphosphate backbone (–$CH_2$–$CH_2$–O–$PO_3$–) as part of the hydrophilic component are reported in Table 1. Based on this consideration, the $HLB_{alk}$ obtained by the Griffin equation reaches 18.6, 18.4 and 17.6, while they were 15.4, 15.2 and 14.7 for the same equation but considering the full polyphosphate block as hydrophobic (Table 1). Due this strong hydrophilic character, it is questionable to see whether these copolymers are able to self-assemble into nanoparticles in aqueous media. It turned out that all the three copolymers synthesized in our work can be directly dissolved in aqueous media (water or phosphate buffer) at room temperature without the help of any organic co-solvent.

**Hydrolytic stability.** Before studying the surfactant properties of the copolymers, the hydrolytic stability of these polyphosphate-based copolymers was investigated in water. As shown in Fig. 2, only the small peak of the triblock copolymers is slightly shifted to lower molecular weight. No shift of the main peak of the SEC traces is observed after 28 days evidencing no significant decrease of molar masses and thus no cleavage of the polyphosphate backbone by hydrolysis under these conditions. So, the diblock copolymers appear stable in milli-Q water at least for 28 days at room temperature, *i.e.* in the conditions used for the following studies.

 

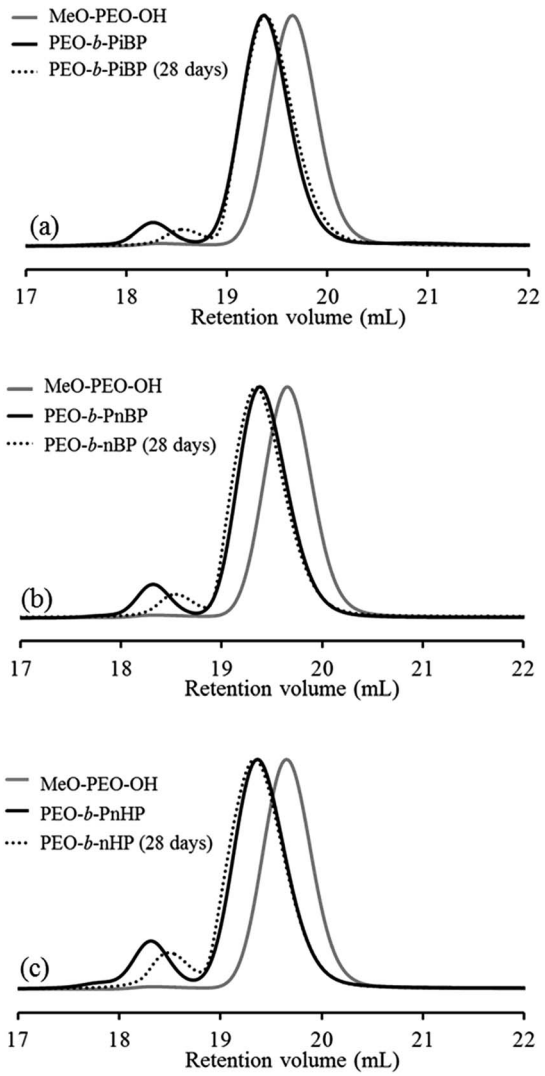


Fig. 2 SEC traces in THF of (a) PEO-*b*-PiBP and MeO-PEO-OH, (b) PEO-*b*-P*n*BP and MeO-PEO-OH and (c) PEO-*b*-P*n*HP and MeO-PEO-OH. The curved dotted line represents the SEC chromatograms of the different copolymers after degradation in milli-Q water.

**Self-assembly in water by dynamic light scattering.** The amphiphilic behaviour of the block copolymers was first investigated by measuring the intensity of scattered light of a concentrated solution for the different copolymers ($3.8 \times 10^{-4}$ mol $L^{-1}$) in milli-Q water. The size and size distribution (PDI) of the diffusers are reported in Table 2 as determined by Dynamic Light Scattering (DLS).

These DLS results show that all the three copolymers directly self-assemble in milli-Q water since diffusers have a size above 16 nm but remaining below 200 nm. Vangeyte *et al.*[34] described the self-assembly of a $PEO_{114}$-*b*-$PCL_8$ copolymer with a comparable DP into micelles with a diameter of about 20 nm. By comparison, the larger diameters observed for the PEO-*b*-PiBP and PEO-*b*-P*n*BP copolymers indicate the formation of loose aggregates rather than well-defined compact core–shell micelles. In contrast, very small and well-defined micelles are observed for the PEO-*b*-P*n*HP copolymer. The spherical morphology was confirmed by Transmission Electron Microscopy (TEM) for PEO-*b*-polyphosphate self-assembled nanoparticles (TEM images in ESI†). As expected, the size of the nanoparticles measured by TEM, *i.e.* under vacuum, appears smaller than the diameter measured by DLS in aqueous medium where the PEO shell is swollen.

**Self-assembly in water by fluorescence spectroscopy.** In order to confirm the formation of hydrophobic pockets above the CAC, pyrene was added to the copolymer solutions of increasing concentration and the pyrene fluorescence spectrum was recorded for each copolymer concentration. Indeed, the fluorescence spectrum of pyrene depends on its environment, especially the intensities of the emission peak at 373 nm (denoted $I_1$), which corresponds to pyrene in aqueous environment, and at 383 nm (denoted $I_3$), corresponding to pyrene in hydrophobic environment, which is the case in the hydrophobic core of the nanoparticles. The measurement of the $I_1/I_3$ ratio as a function of the logarithm of copolymer concentration is shown in the ESI.† From the slope break of these curves, the CAC could be obtained for the three copolymers (Table 2). This pyrene experiment confirms the presence of self-assembled nanoparticles of the three PEO-*b*-polyphosphate copolymers above a given concentration depending on the length of the polyphosphate pendant groups.

In line with the recent report of Yang *et al.*,[31] we can conclude that the CAC decreases when the length of the pendant groups increases and thus when the hydrophobicity of the polyphosphate block increases. In addition, varying the architecture of the alkyl side-chain from iso-butyl to *n*-butyl appears to decrease slightly the nanoparticles size and increase the CAC of the copolymer of identical HLB. Remarkably, the used copolymers are able to self-assemble in water without the help of organic co-solvent in contrast to the report of Yang *et al.*[31] on PEO-*b*-polyphosphate and to PEO-*b*-PCL copolymers as reported by Cajot *et al.*[10]

It is noteworthy that above the CAC, the size of the assemblies varies slightly with the concentration. The size generally decreases when increasing the concentration (Table 2, compares columns 2 and 4) except for the iBP based copolymer. However, no dramatic changes of the nanoparticles size are observed with the concentration by diluting or increasing it above the CAC.

## Behaviour of the PEO-*b*-polyphosphate at the air–water interface

The self-association in water of the diblock copolymers being demonstrated, the comparative ability to reduce the air–water interfacial tension was measured in function of the copolymer concentration. For all the three copolymers, a clear decrease of the interfacial tension is observed upon increasing the copolymer concentration (Fig. 3). A clear break in the slope is observed in each case which occurs for quite similar concentration for both butyl polyphosphate ($\sim 3 \times 10^{-6}$ mol $L^{-1}$) and corresponds to a levelling of the interfacial tension down to 30 mN $m^{-1}$.

Table 2 Hydrodynamic diameter ($D_h$) and size distribution (PDI) of the PEO-*b*-polyphosphate assemblies in milli-Q water, determined by DLS measured [a]for a copolymer concentration of $1.9 \times 10^{-4}$ mol $L^{-1}$ and [b]for a copolymer concentration of $3.8 \times 10^{-4}$ mol $L^{-1}$, [c]CAC values determined by pyrene probe fluorescence spectroscopy and [d]the SCC values by tensiometry

| Copolymers | $D_h$[a] (nm) | PDI[a] | $D_h$[b] (nm) | PDI[b] | CAC[c] (mol $L^{-1}$) | SCC[d] (mol $L^{-1}$) |
|---|---|---|---|---|---|---|
| PEO-*b*-PiBP | 153 ± 2 | 0.114 | 169 ± 3 | 0.098 | $3.1 \times 10^{-5}$ | $4.1 \times 10^{-6}$ |
| PEO-*b*-P*n*BP | 145 ± 2 | 0.189 | 126 ± 3 | 0.168 | $4.6 \times 10^{-5}$ | $2.2 \times 10^{-6}$ |
| PEO-*b*-P*n*HP | 21 ± 2 | 0.224 | 16 ± 4 | 0.098 | $2.8 \times 10^{-6}$ | $2.8 \times 10^{-7}$ |

In the case of PEO-*b*-P*n*HP copolymer, this break appears at a concentration of one order of magnitude lower ($\sim 3 \times 10^{-7}$ mol $L^{-1}$) as compared for PEO-*b*-PiBP and PEO-*b*-P*n*BP in line with the lower CAC measured by pyrene fluorescence analysis. It is noteworthy that for PEO-*b*-P*n*HP copolymer, the interfacial tension does not stabilize after the slope break. It rather keeps decreasing slowly when we further increase the concentration, the interfacial tension remaining above 35 mN $m^{-1}$.

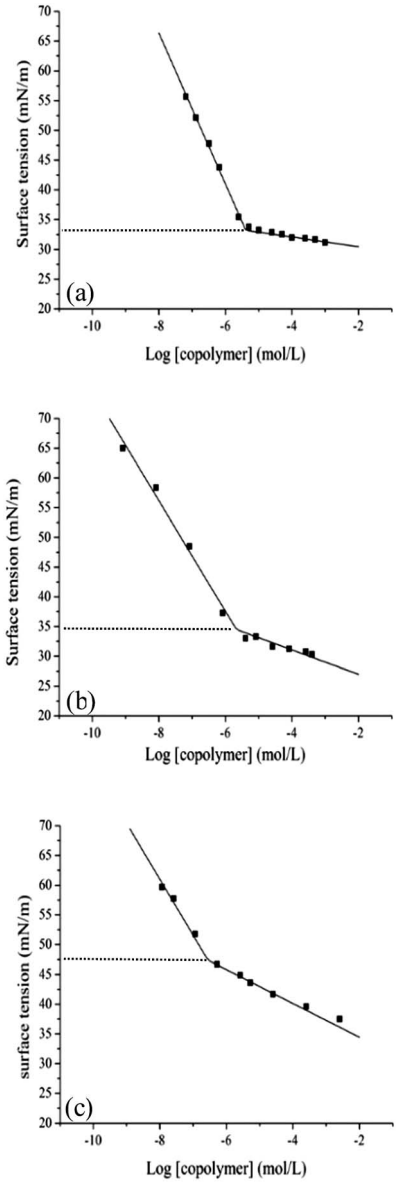


Fig. 3 Plots of surface tension *versus* log[copolymer] for the PEO-*b*-polyphosphate copolymers: (a) PEO-*b*-PiBP, (b) PEO-*b*-P*n*BP and (c) PEO-*b*-P*n*HP.

These slope change concentration (SCC) values were compared with PEO-*b*-PCL amphiphilic block copolymer presenting a similar DP for each block. Vangeyte *et al.*[35] determined by tensiometry the SCC value for $PEO_{114}$-*b*-$PCL_8$ copolymers which is approximately $8 \times 10^{-6}$ mol $L^{-1}$. This value is similar than the SCC values for $PEO_{114}$-*b*-$PiBP_9$ and $PEO_{114}$-*b*-P*n*$BP_9$ copolymers whereas the SCC value for the most hydrophobic *n*HP system is much lower. Comparing the surface tension values at the slope break with those for the $PEO_{114}$-*b*-$PCL_8$ copolymers ($\sim$51 mN $m^{-1}$),[35] we observe that the surface tension values for the PEO-*b*-polyphosphate at the slope break are much lower, approximately 35 mN $m^{-1}$ for PEO-*b*-PiBP and PEO-*b*-P*n*BP copolymers and 47 mN $m^{-1}$ for the most hydrophobic *n*HP system, showing the higher efficiency of PEO-*b*-polyphosphate copolymers to stabilize the air–water interface as compared to the PEO-*b*-PCL of the same DP.

## Conclusion

This study demonstrated that the amphiphilic block copolymers ($PEO_{114}$-*b*-$PiBP_8$, $PEO_{114}$-*b*-P*n*$BP_9$ and $PEO_{114}$-*b*-P*n*$HP_8$) are able to self-assemble in water into nanoparticles without the use of any organic co-solvent whatever the length of the pendant group along the polyphosphate block and thus whatever the hydrophobicity of the polyphosphate block. The surfactant properties of these copolymers including aqueous micellization and air–water interfacial tension investigations were systematically studied. The CAC decreases when the length of the pendant group increases and thus when the polyphosphate block is more hydrophobic. Accordingly, a low CAC can be achieved with a heptyl chain. In addition, we evidenced that the architecture of the alkyl chain while keeping constant the HLB has an effect on the size and CAC of the self-assemblies even if the particles size remains below 200 nm in any case. The copolymers were synthesized by metal-free ring-opening polymerization of the corresponding cyclic phosphates initiated by a PEO macro-initiator. Such copolymers appear thus as a promising class of environmental-friendly neutral surfactant copolymers of interest in various fields of applications such as food, cosmetic, biomedical and detergency applications.

 

# Experimental

## Materials

2-Chloro-1,3,2-dioxaphospholane 2-oxide (COP, Acros), methanol (MeOH, Acros), diethyl ether (Chem-lab) and calcium hydride ($CaH_2$, Aldrich) were used as received without further purification. 2-Methylpropan-1-ol (Aldrich), butan-1-ol (Aldrich), heptan-1-ol (Alfa Aesar), *N*,*N*-diethylethanamine (triethylamine, TEA, Aldrich) and 1,8-diazabicyclo [5.4.0]undec-7-ene (DBU, Aldrich) were dried over $CaH_2$ at room temperature and purified by distillation under reduced pressure just before use. Toluene (Chem-lab), tetrahydrofuran (THF, Chem-lab) and dichloromethane ($CH_2Cl_2$, Chem-lab) were dried on molecular sieves. Monomethoxy-PEO (MeO-PEO-OH, $M_n$ = 5000 g mol$^{-1}$, Aldrich) was dried by three azeotropic distillations with anhydrous toluene before use. Milli-Q water was used for the micelle's preparation. 1-1-[3,5-Bis(trifluoromethyl)phenyl]-3-cyclohexyl-2-thiourea (TU), 2-(2-methylpropoxy)-1,3,2-dioxaphospholane 2-oxide (iBP) and 2-butoxy-1,3,2-dioxaphospholane 2-oxide (*n*BP) monomers were synthesized as described in the literature elsewhere.[21,31,37]

## Structural characterization techniques

$^1$H and $^{31}$P NMR analyses were performed on a Bruker Advance 250 MHz spectrometer in $CDCl_3$ at 25 °C in the FT mode. The $^{31}$P NMR measurement was carried out with the $^1$H powergate decoupling method using a 30° flip angle. $^1$H NMR chemical shifts are reported in ppm relative to $Me_4Si$. $^{31}$P NMR chemical shifts are reported in ppm relative to $H_3PO_4$. Size exclusion chromatography (SEC) was carried out in THF at 45 °C at a flow rate of 0.7 mL min$^{-1}$ with Viscotek 305 TDA liquid chromatograph. The PL gel 5 μm ($10^4$ Å, $10^3$ Å and 100 Å) columns were calibrated with PEO standards.

## Synthetic procedures

**Monomer synthesis.** 2-Heptyloxy-1,3,2-dioxaphospholane 2-oxide (*n*HP) was synthesized by the esterification reaction of COP with 1-heptanol in the presence of TEA. Typically, COP (100 g, 0.702 mol) in a THF solution (200 mL) was added dropwise, under stirring at 0 °C, to a solution of the anhydrous alcohol and TEA in dry THF (200 mL) (COP/TEA/alcohol = 1/1/1). After the complete addition, the solution was stirred at 0 °C for 4 hours and the resulting mixture was filtrated to remove the alkyl ammonium salt before concentrating the filtrate under vacuum. Finally, the monomer was purified by fractional distillation under vacuum ($10^{-4}$ Torr, $T_b$ = 105 °C, yield = 53%).

$^1$H NMR (250 MHz, $CDCl_3$, 25 °C, TMS): 0.9 ppm (t, 3H, –$CH_2$–C$H_3$), 1.3 ppm (t, 8H, –O–$CH_2$–$CH_2$–(C$H_2$)$_4$–$CH_3$), 1.7 ppm (m, 2H, –O–$CH_2$–C$H_2$–$(CH_2)_4$–$CH_3$), 4.1 ppm (dt, $^2J_{HH}$ = 6.6 Hz and $^3J_{PH}$ = 8.6 Hz, 2H, –O–C$H_2$–$CH_2$–$(CH_2)_4$–$CH_3$), 4.4 ppm (m, 4H, –O–C$H_2$–C$H_2$–O–). $^1$H-decoupled $^{31}$P NMR ($CDCl_3$, 101 MHz): 18.1 ppm.

**Polymerization from a PEO macro-initiator.** The polymerization of *n*BP, iBP or *n*HP was performed in $CH_2Cl_2$ at 0 °C with MeO-PEO-OH as a macro-initiator, DBU as a catalyst and TU as a co-catalyst with a ratio $[PEO\text{-}OH]_0/[monomer]_0/[DBU]_0/[TU]_0$ = 1/10/1.3/0.5. In a glass reactor, TU (386 mg, 1.04 mmol) and the cyclic phosphate monomer (20.8 mmol) were dried by three successive azeotropic distillations with toluene and dissolved in $CH_2Cl_2$ ($[monomer]_0$ = 1 mol L$^{-1}$) before being transferred under inert atmosphere into a second glass reactor containing 10 g (2.1 mmol) of MeO-PEO-OH, freshly dried by three azeotropic distillations. After complete solubilisation of PEO, 0.4 mL of DBU (2.7 mmol) was added under nitrogen atmosphere with a freshly flamed stainless steel capillary. After 60 minutes of polymerization (after 70 minutes for *n*HP), the solution was concentrated under vacuum and the polymer was precipitated in cold diethyl ether and filtrated. Residual DBU was eliminated overnight by dialysis against MeOH (Spectrum, membrane porosity = 1000 g mol$^{-1}$). After elimination of MeOH under vacuum, the residue was dissolved in THF and the amphiphilic copolymer was recovered by precipitation in cold diethyl ether before being dried under vacuum.

*For PEO-b-PnBP.* The $^1$H NMR spectrum is in good agreement with the reported spectrum by Yang *et al.*[31] $^1$H-decoupled $^{31}$P NMR (101 mHz, $CDCl_3$, 25 °C): −0.60 ppm. $M_w/M_n$ (SEC) = 1.10.

*For PEO-b-PiBP.* $^1$H NMR (250 MHz, $CDCl_3$, 25 °C, TMS): 0.95 ppm (d, 6H, –CH–(C$H_3$)$_2$), 1.95 ppm (m, 1H, –C*H*–$(CH_3)_2$), 3.65 ppm (s, 4H, –C–O–C$H_2$–C$H_2$–O–C–), 3.85 ppm (m, 2H, –O–C$H_2$–CH–$(CH_3)_2$), 4.3 ppm (m, 4H, –P–O–C$H_2$–C$H_2$–O–P–). $^1$H-decoupled $^{31}$P NMR (101 mHz, $CDCl_3$, 25 °C): −0.60 ppm. $M_w/M_n$ (SEC) = 1.10.

*For PEO-b-PnHP.* $^1$H NMR (250 MHz, $CDCl_3$, 25 °C, TMS): 0.9 ppm (t, 3H, –$CH_2$–C$H_3$), 1.3 ppm (m, 8H, –O–$CH_2$–$CH_2$–(C$H_2$)$_4$–$CH_3$), 1.7 ppm (m, 2H, –O–$CH_2$–C$H_2$–$(CH_2)_4$–$CH_3$), 3.65 ppm (s, 4H, –C–O–C$H_2$–C$H_2$–O–C–), 4.1 ppm (m, 2H, –O–C$H_2$–$CH_2$–$(CH_2)_4$–$CH_3$), 4.25 ppm (m, 4H, –P–O–C$H_2$–C$H_2$–O–P–). $^1$H-decoupled $^{31}$P NMR (101 mHz, $CDCl_3$, 25 °C): −0.60 ppm. $M_w/M_n$ (SEC) = 1.10.

## Characterization of the copolymer in water

**Hydrolytic stability.** The hydrolytic stability of the copolymers was monitored in Milli-Q water at room temperature over a period of 1, 7, 14 and 28 days. 100 mg of copolymer were dissolved in 35 mL of Milli-Q water. The concentration of the polymer was set at 3 mg mL$^{-1}$. At the predetermined times, 3 mL of the solution were collected, dried by lyophilisation before being analysed by SEC in THF.

**Dynamic light scattering (DLS).** Typically, 25 mg or 50 mg of the PEO-*b*-polyphosphate copolymer were directly dissolved in 20 mL deionized water and stirred overnight. Particle size and size distribution were acquired from freshly prepared copolymer solutions by dynamic light scattering (DLS). DLS measurements were performed using a Beckman Coulter Delsa Nano C Particle Analyzer and the data were treated by the Delsa Nano UI 2.21 software. The average size distribution of aqueous micellar solutions was determined based on the CONTIN method. All the measurements were carried out in a glass cell at 25 °C at a measuring angle of 165°. Aqueous micellar solutions were filtered with a microfilter having an average pore size of 1.2 μm. All DLS measurements were repeated five times in order to check their reproducibility.

**Transmission electron microscopy (TEM).** The samples for TEM were prepared by slow evaporation of the copolymer aqueous solutions after DLS analysis on a formvar-coated grid. The excess of solutions was removed with a filter paper. The samples were analysed with a Philips CM100 microscope equipped with an Olympus camera and transferred to a computer equipped with a Megaview system.

**Fluorescence spectroscopy measurements.** CAC values in milli-Q water for the different amphiphilic block copolymers were determined by the pyrene probe fluorescence spectroscopy using a LS50B luminescence spectrometer (Perkin Elmer). Typically, solid pyrene ($2.6 \times 10^{-8}$ mol) was dissolved in aqueous solutions of the amphiphilic copolymer of increasing concentration from $1 \times 10^{-10}$ to $1 \times 10^{-3}$ mol $L^{-1}$. Milli-Q water was used to dissolve first the copolymer before adding it to vials containing the pyrene. Since the amount of needed pyrene is quite low (5.2 μg), a solution of pyrene ($1.3 \times 10^{-3}$ mol $L^{-1}$) in acetone was first prepared. 20 μL of the pyrene solution was transferred into glass vials and acetone was evaporated at room temperature before adding copolymer solution. After one night of stirring at room temperature, the fluorescence spectra of pyrene were recorded from 360 to 460 nm after an excitation at 339 nm. The emission and excitation slit widths were set at 2.5 and 3.0, respectively. The ratio of the peak intensities at 373 nm and 383 nm ($I_{373}/I_{383}$) of the emission spectra were calculated for each copolymers solution and recorded as a function of the copolymer concentration.

### Characterization of the air–water interface by tensiometry

The rising air-bubble method was used to study the efficiency of the PEO-*b*-polyphosphates copolymers to stabilize the air–water interface. Aqueous solutions of different copolymer concentrations ranging from $10^{-10}$ to $10^{-3}$ mol $L^{-1}$ were prepared before being tested by a Tracker tensiometer (TECLIS, France). The method based on the analysis of a 5 μL air bubble deformation affords to measure the air–water interfacial tension at the equilibrium of adsorption for each copolymer.

## Acknowledgements

This study was performed within the Interreg Euregio Meuse-Rhin IV-A consortium BioMIMedics (2011–2014). The University of Liege (Belgium), Maastricht University (The Netherlands), University of Hasselt (Belgium), RWTH Aachen (Germany), and Fachhochschule Aachen (Germany) together with several local small biotechnological enterprises cooperate in BioMIMedics. This particular study was financed through generous contributions of the European Union (through Interreg IV-A), the government of Wallonia (Belgium), and the "Provincie Nederlands Limburg" (The Netherlands). CERM is much indebted to IAP VII-05 "Functional Supramolecular Systems" (FS). P.L. is Research Associate by the FRS-FNRS.

## Notes and references

1 L. L. Schramm, E. N. Stasiuk and D. G. Marangoni, *Annu. Rep. Prog. Chem., Sect. C: Phys. Chem.*, 2003, **99**, 3–48.
2 M. Moradi and Y. Yamini, *J. Sep. Sci.*, 2012, **35**, 2319–2340.
3 P. A. Ash, C. D. Bain and H. Matsubara, *Curr. Opin. Colloid Interface Sci.*, 2012, **17**, 196–204.
4 J. Texter, *Curr. Opin. Colloid Interface Sci.*, 2014, **19**, 163–174.
5 C. Boyère, A. F. Léonard, B. Grignard, A. Favrelle, J. P. Pirard, M. Paquot, C. Jérôme and A. Debuigne, *Chem. Commun.*, 2012, **48**, 8356–8358.
6 X. B. Xiong, Z. Binkhathlan, O. Molavi and A. Lavasanifar, *Acta Biomater.*, 2012, **8**, 2017–2033.
7 M. J. Kositza, C. Bohne, P. Alexandridis, T. A. Hatton and J. F. Holzwarth, *Macromolecules*, 1999, **32**, 5539–5551.
8 H. Y. Liu, S. Prévost and M. Gradzielski, *Z. Phys. Chem.*, 2012, **226**, 675–694.
9 J. Rieger, C. Passirani, J. P. Benoit, K. Van Butsele, R. Jérôme and C. Jérôme, *Adv. Funct. Mater.*, 2006, **16**, 1506–1514.
10 S. Cajot, P. Lecomte, C. Jérôme and R. Riva, *Polym. Chem.*, 2013, **4**, 1025–1037.
11 J. K. Oh, *Soft Matter*, 2011, **7**, 5096–5108.
12 Z. Zhu, *Biomaterials*, 2013, **34**, 10238–10248.
13 E. Olkowska, Z. Polkowska and J. Namieśnik, *Chem. Rev.*, 2011, **111**, 5667–5700.
14 G. P. Kumar and P. Rajeshwarrao, *Acta Pharm. Sin. B*, 2011, **1**, 208–219.
15 B. A. Kerwin, *J. Pharm. Sci.*, 2008, **97**, 2924–2935.
16 K. Kałuzyński, J. Libiszowski and S. Penczek, *Macromolecules*, 1976, **9**, 365–367.
17 J. Libiszowski, K. Kaluzynski and S. Penczek, *J. Polym. Sci., Polym. Chem. Ed.*, 1978, **16**, 1275–1283.
18 Y. C. Wang, S. Y. Shen, Q. P. Wu, D. P. Chen, J. Wang, G. Steinhoff and N. Ma, *Macromolecules*, 2006, **39**, 8992–8998.
19 C. S. Xiao, Y. C. Wang, J. Z. Du, X. S. Chen and J. Wang, *Macromolecules*, 2006, **39**, 6825–6831.
20 Y. Iwasaki and E. Yamaguchi, *Macromolecules*, 2010, **43**, 2664–2666.
21 B. Clément, B. Grignard, L. Koole, C. Jérôme and P. Lecomte, *Macromolecules*, 2012, **45**, 4476–4486.
22 J. Baran and S. Penczek, *Macromolecules*, 1995, **28**, 5167–5176.
23 N. Narendran and K. Kishore, *J. Appl. Polym. Sci.*, 2003, **87**, 626–631.
24 Y. C. Wang, L. Y. Tang, Y. Li and J. Wang, *Biomacromolecules*, 2009, **10**, 66–73.
25 S. Zhang, J. Zou, M. Elsabahy, A. Karwa, A. Li, D. A. Moore, R. B. Dorshow and K. L. Wooley, *Chem. Sci.*, 2013, **4**, 2122–2126.
26 Z. Zhao, J. Wang, H. Q. Mao and K. W. Leong, *Adv. Drug Delivery Rev.*, 2003, **55**, 483–499.
27 Y. Tao, J. He, M. Zhang, Y. Hao, J. Liu and P. Ni, *Polym. Chem.*, 2014, **5**, 3443.
28 Y. Zhang, J. He, D. Cao, M. Zhang and P. Ni, *Polym. Chem.*, 2014, **5**, 5124.
29 Y. C. Wang, Y. Y. Yuan, J. Z. Du, X. Z. Yang and J. Wang, *Macromol. Biosci.*, 2009, **9**, 1154–1164.
30 J. Wang, Y. Y. Yuan and J. Z. Du, *Polymer Science: A Comprehensive Reference*, Elsevier, 2012, vol. 4.

 

31 C.-Y. Sun, Y.-C. Ma, Z.-Y. Cao, D.-D. Li, F. Fan, J.-X. Wang, W. Tao and X.-Z. Yang, *ACS Appl. Mater. Interfaces*, 2014, **6**, 22709–22718.
32 K. Sumida, Y. Igarashi, N. Toritsuka, T. Matsushita, K. Abe-Tomizawa, M. Aoki, T. Urushidani, H. Yamada and Y. Ohno, *Hum. Exp. Toxicol.*, 2011, **30**, 1701–1709.
33 X. Zhai, W. Huang, J. Liu, Y. Pang, X. Zhu, Y. Zhou and D. Yan, *Macromol. Biosci.*, 2011, **11**, 1603–1610.
34 P. Vangeyte, S. Gautier and R. Jérôme, *Colloids Surf., A*, 2004, **242**, 203–211.
35 P. Vangeyte, B. Leyh, M. Heinrich, J. Grandjean, C. Bourgaux and R. Jérôme, *Langmuir*, 2004, **20**, 8442–8451.
36 Y. Ohya, A. Takahashi and K. Nagahama, *Adv. Polym. Sci.*, 2012, **247**, 65–114.
37 R. C. Pratt, B. G. G. Lohmeijer, D. A. Long, P. N. P. Lundberg, A. P. Dove, H. Li, C. G. Wade, R. M. Waymouth and J. L. Hedrick, *Macromolecules*, 2006, **39**, 7863–7871.